AGU PUBLICATIONS

JGR

Journal of Geophysical Research: Atmospheres

RESEARCH ARTICLE
10.1002/2016JD025999

Key Points:
- Oxidation state of alpha-pinene SOA increases with increasing seed surface area
- Alpha-pinene SOA is more oxidized in the presence of nitrate-containing seed aerosol than with ammonium sulfate seed aerosol

Supporting Information:
- Supporting Information S1

Correspondence to:
C. K. Chan and J. H. Seinfeld,
chak.k.chan@cityu.edu.hk;
seinfeld@caltech.edu

Citation:
Huang, D. D., X. Zhang, N. F. Dalleska, H. Lignell, M. M. Coggon, C.-M. Chan, R. C. Flagan, J. H. Seinfeld, and C. K. Chan (2016), A note on the effects of inorganic seed aerosol on the oxidation state of secondary organic aerosol —α-Pinene ozonolysis, *J. Geophys. Res. Atmos.*, *121*, 12,476–12,483, doi:10.1002/2016JD025999.

Received 25 SEP 2016
Accepted 10 OCT 2016
Accepted article online 12 OCT 2016
Published online 31 OCT 2016

A note on the effects of inorganic seed aerosol on the oxidation state of secondary organic aerosol—α-Pinene ozonolysis

Dan Dan Huang[1], Xuan Zhang[2,3], Nathan F. Dalleska[2], Hanna Lignell[4,5], Matthew M. Coggon[4,6], Chi-Ming Chan[1,7], Richard C. Flagan[2,4], John H. Seinfeld[2,4], and Chak K. Chan[1,7,8]

[1]Department of Chemical and Biomolecular Engineering, Hong Kong University of Science and Technology, Hong Kong, China, [2]Division of Engineering and Applied Science, California Institute of Technology, Pasadena, California, USA, [3]Now at Aerodyne Research Inc., Billerica, Massachusetts, USA, [4]Division of Chemistry and Chemical Engineering, California Institute of Technology, Pasadena, California, USA, [5]Now at South Coast Air Quality Management District, Diamond Bar, California, USA, [6]Now at Earth System Research Laboratory, National Oceanic and Atmospheric Administration, Boulder, Colorado, USA, [7]Division of Environment, Hong Kong University of Science and Technology, Hong Kong, China, [8]School of Energy and Environment, City University of Hong Kong, Hong Kong, China

Abstract We compare the oxidation state and molecular composition of α-pinene-derived secondary organic aerosol (SOA) by varying the types and surface areas of inorganic seed aerosol that are used to promote the condensation of SOA-forming vapors. The oxidation state of α-pinene SOA is found to increase with inorganic seed surface area, likely a result of enhanced condensation of low-volatility organic compounds on particles versus deposition on the chamber wall. α-Pinene SOA is more highly oxygenated in the presence of sodium nitrate (SN) seed than ammonium sulfate seed. The relative abundance of semivolatile monomers and low-volatility dimer components that account for more than half of α-pinene SOA mass is not significantly affected by the composition of seed aerosol. Enhanced uptake of highly oxidized small carboxylic acids onto SN seed particles is observed, which could potentially explain the observed higher SOA oxidation state in the presence of SN seed aerosol. Overall, our results demonstrate that a combined effect of seed aerosol composition and surface area leads to an increase in the O:C atomic ratio of α-pinene SOA by as much as a factor of 2.

1. Introduction

Environmental chambers are a principal means to study the formation of secondary organic aerosol (SOA) from photooxidation of volatile organic compounds (VOCs). Chamber studies are often carried out with seed particles such as ammonium sulfate to promote the condensation of SOA-forming organic vapors. Under dry and neutral conditions, inorganic seed particles are assumed to act as an inert medium that is internally well mixed with the organic components. The effect of acidified seed particles on SOA production has been the subject of a number of studies, and the importance of acid-catalyzed heterogeneous reactions on particle oligomer content has been widely recognized [*Jang et al.*, 2002, 2003; *Surratt et al.*, 2007; *Gaston et al.*, 2014, and references herein]. Increasing evidence has also revealed the role of hydrated seed particles on SOA production not only through physical dissolution of water-soluble species but also via hydrolysis of reactive intermediates in the aqueous phase [e.g., *Nguyen et al.*, 2014]. Limited studies have investigated the effects of inorganic seed levels and types on SOA chemical properties [*Hao et al.*, 2007; *Lu et al.*, 2009]. Recent studies have reported increasing SOA mass corresponding to increasing initial seed surface area, suggesting that condensation of SOA-forming vapors onto seed particles cannot be simply explained by instantaneous equilibrium gas-particle partitioning. Particle-phase mass transfer potentially plays an important role in controlling the condensation rate of various SOA components [*Zhang et al.*, 2014; *Mai et al.*, 2015; *McVay et al.*, 2016].

Here we report a series of experiments to examine the effects of the level and type of inorganic seed particles on the chemical composition of SOA from ozonolysis of α-pinene. High-resolution aerosol mass spectrometry (AMS), ultra performance liquid chromatography/electrospray ionization quadrupole time-of-flight mass spectrometry (UPLC/ESI-ToFMS), and time-of-flight secondary ion mass spectrometry (ToF-SIMS) are employed to probe differences in the average carbon oxidation state $\left(\overline{OS_C}\right)$ and molecular composition of α-pinene SOA in the presence of two types of seed particles at varying surface areas.

2. Experimental

All experiments were performed in Caltech's dual 24 m^3 Teflon environmental chambers. Before each experiment, the chamber was flushed for > 24 h until particle number concentration was < 10 cm^{-3} and the volume concentration was < 0.01 μm^3 cm^{-3}. Temperature, relative humidity, ozone, and NO_x were continuously monitored. α-Pinene (~50 ppb) was oxidized by O_3 (~100 ppb) in the presence of ammonium sulfate (AS) or sodium nitrate (SN) seed particles under low (~1×10^3 μm^2 cm^{-3}), medium (~3×10^3 μm^2 cm^{-3}), and high (~5×10^3 μm^2 cm^{-3}) seed surface area, respectively. Seed aerosols were generated by atomizing an aqueous solution with a constant-rate atomizer and passed directly into the chamber. Experimental conditions and initial seed surface area as measured by a custom-built Scanning Mobility Particle Sizer are summarized in Table S1. Experiments were performed in the presence of cyclohexane, serving as an OH scavenger, at a mixing ratio of 22 ppm. During each experiment, offline aerosol samples were collected through a 1 m charcoal denuder with a single-stage Sioutas cascade impactor [*Sioutas*, 2004] (0.25 μm cut point at 9 L min^{-1} collection flow) and a 25 mm CaF_2 window as the impaction substrate.

Chamber aerosols were sampled continuously by an AMS. The AMS was operated alternately between V mode and W mode for 1 min each. Standard AMS data analysis toolkits SQUIRREL v1.56D and PIKA 1.15D based on Igor Pro (6.32A) were utilized to process the V mode and W mode data, respectively. The "improved-ambient" elemental analysis method for AMS spectra is utilized in this study [*Canagaratna et al.*, 2015]. To obtain values of f_{CO2} and f_{CHO} required in the improved-ambient method, background corrections for gas CO_2^+ signal and $^{15}N^{14}N^+$ fragments were made to all the data sets by sampling the chamber air through a particle filter before the injection of α-pinene. *Pieber et al.* [2016] recently found that inorganic salts can induce CO_2 production when impinging on the heated tungsten vaporizer utilized by the AMS due to oxidation of predeposited refractory carbon. The non-OA induced CO_2^+ signal (1%) is close to the lower bound of the range (0.4% ~ 10%) in *Pieber et al.* [2016]. The interference is calibrated and evaluated in Text S1 in the supporting information. Bias in the elemental ratio is not observed, likely because the Caltech Chamber AMS was never used in field measurements, avoiding contamination by crustal organic materials. UPLC/ESI-ToFMS and gas chromatography/mass spectrometry (GC/MS) were used to characterize particulate molecular identities. Details about optimal operation of the instruments can be found in SI S2 and S3.

Flow cell experiments are detailed in Text S4. Briefly, droplets of AS or SN were deposited onto a silicon wafer coated with Au by an autopipette and placed in a stainless steel cell, drying for > 2 h under high-purity N_2 gas. The VOC vapor (acetic acid) at ~1 ppm was introduced to the cell containing the substrate and deposited materials at a flow of ~1 L min^{-1} to react for ~17 h. Particles on the substrate were immediately analyzed by time-of-flight secondary ion mass spectrometry (ToF-SIMS) to estimate the relative thicknesses of the acetic acid layer on the surface of the AS and SN particles.

3. Results and Discussion

3.1. Effect of Seed Concentration on Average Carbon Oxidation State $(\overline{OS_C})$

Average carbon oxidation state $(\overline{OS_C})$ is a measure of the degree of oxidation of atmospheric aerosols [*Kroll et al.*, 2011]. Figure 1a summarizes the $\overline{OS_C}$ of α-pinene ozonolysis SOA as measured by the AMS in AS- and SN-seeded experiments at different initial seed surface areas. Decay rates of gas-phase α-pinene are the same for all experiments (Figure 1b). The SOA formed in the absence of seed aerosol ("nucleation" in Figure 1a) exhibits the lowest oxidation state among all the experiments. $\overline{OS_C}$ increases with seed surface area in both AS- and SN-seeded experiments. The dependence of $\overline{OS_C}$ on the seed surface area can be explained by the competition between condensation of SOA-forming vapors onto suspended particles and the chamber wall. The relative importance of these two processes can be evaluated from the estimated timescale to establish vapor-particle ($\tau_{v,p}$) and vapor-wall ($\tau_{v,w}$) equilibrium partitioning (Figure 2). Details of timescale estimation are presented in *Zhang et al.* [2015b] and are also given in Text S5.

Figure 2 shows the estimated vapor-particle equilibrium partitioning timescale ($\tau_{v,p}$), ranging from ~1 min to ~100 min as a function of the particle accommodation coefficient (α_p) under different initial seed surface areas. As the seed surface area increases, the timescale for vapor-particle equilibrium partitioning decreases by a factor of ~5. Also shown in Figure 2 is the predicted vapor-wall equilibrium partitioning timescale ($\tau_{v,w}$)

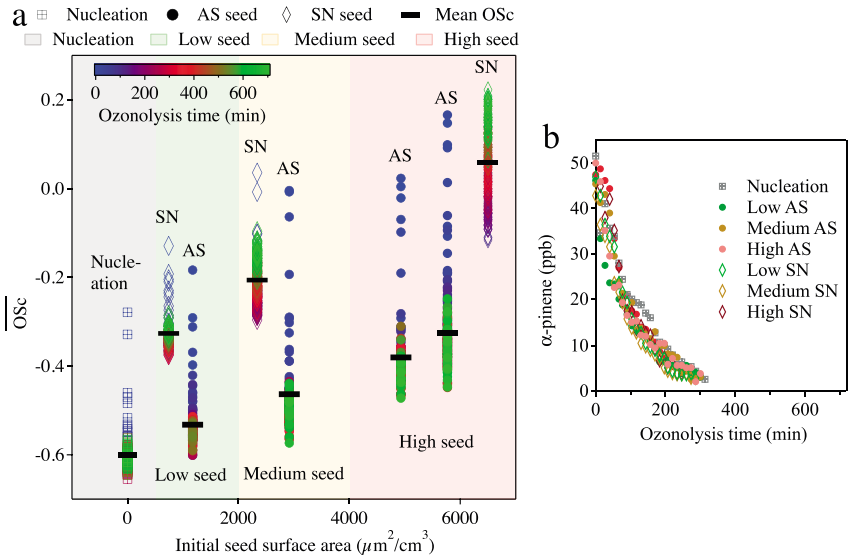

Figure 1. (a) Oxidation state $\left(\overline{OS_C} = 2\times O/C\text{-}H/C\right)$ as a function of initial seed aerosol surface area in nucleation, AS- and SN-seeded experiments; (b) GC-FID measured decay of α-pinene under all seed conditions.

for two monomers, i.e., $C_{10}H_{16}O_3$ (pinonic acid) and $C_8H_{12}O_4$ (terpenylic acid), and two dimers, i.e., $C_{19}H_{28}O_7$ and $C_{19}H_{28}O_9$. These four species were detected in the offline LC/MS analysis (Figure 3) and can be considered as representative semivolatile organic compounds (SVOCs) and extremely low volatility organic compounds (ELVOCs) in the α-pinene SOA system [*Zhang et al.*, 2015a]. The predicted timescale associated with vapor-wall partitioning of SVOCs (e.g., ~770 min and ~450 min for $C_{10}H_{16}O_3$ and $C_8H_{12}O_4$, respectively) significantly exceeds that estimated for establishing vapor-particle equilibrium partitioning ($\tau_{v,p}$ ~1–100 min). As a consequence, the condensation of SVOCs onto suspended particles is essentially unaffected by the magnitude of the initial seed surface area. In contrast, the estimated vapor-wall partitioning timescale for extremely low volatility organic compounds (ELVOCs) (e.g., ~40 min and ~35 min for $C_{19}H_{28}O_7$ and $C_{19}H_{28}O_9$, respectively) is comparable to that associated with vapor-particle equilibrium partitioning. As a result, at increasing seed surface area, a fraction of ELVOC vapors that would have deposited onto the wall condense preferentially onto suspended particles. Overall, an increase in the initial seed surface area results in accelerated condensation of low volatility organic compounds and ELVOCs onto particles potentially increasing $\overline{OS_C}$ but with little effect from most SVOCs.

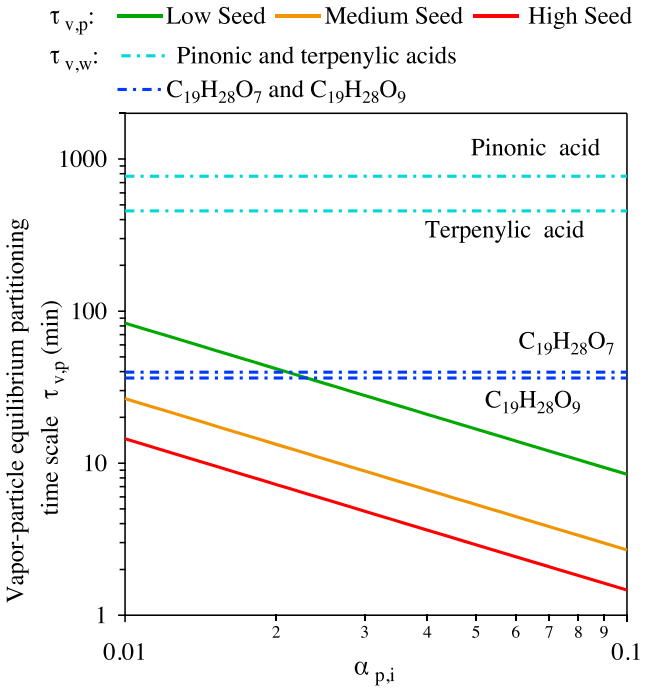

Figure 2. Comparison of estimated vapor-particle ($\tau_{v,p}$) and vapor-wall ($\tau_{v,w}$) equilibration timescale. Green, yellow, and red solid lines represent vapor-particle equilibration timescale as function of vapor mass accommodation coefficients on particles (α_p) under low, medium, and high seed conditions, respectively. The blue dashed lines represent vapor-wall equilibration timescale of SVOCs (light blue, $C_8H_{12}O_4$ and $C_{10}H_{16}O_3$, and ELVOCs (dark blue, $C_{19}H_{28}O_7$ and $C_{19}H_{28}O_9$).

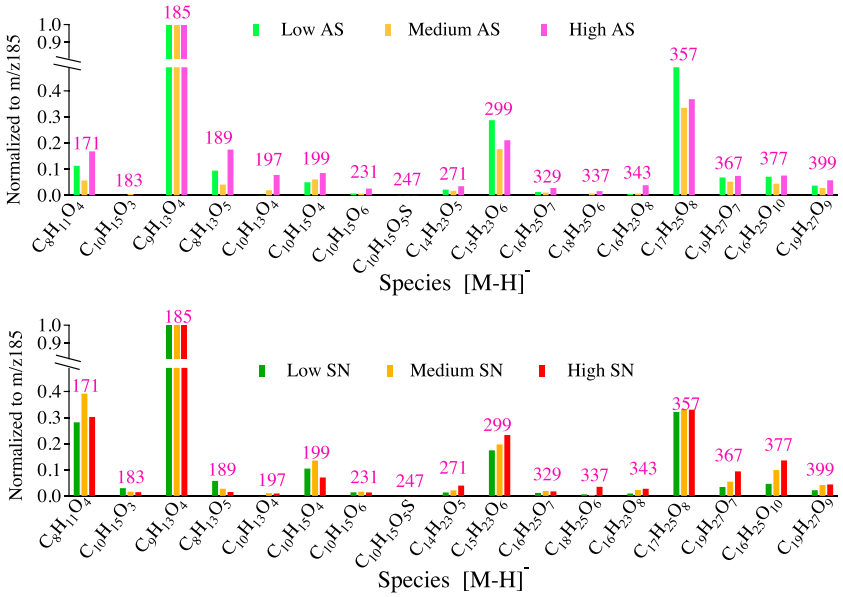

Figure 3. Relative abundance of products (defined as the ratio of mass concentration of specific compound to the concentration of pinic acid, $[C_9H_{13}O_4]^-$, m/z 185) detected in the (top) AS and (bottom) SN offline extracts under different seed surface areas. Compounds with formula $C_{8\text{-}10}H_{12\text{-}16}O_{3\text{-}6}$ are monomers and with $C_{14\text{-}19}H_{24\text{-}28}O_{5\text{-}10}$ are dimers.

We note that the predicted timescale associated with vapor-wall partitioning of these α-pinene oxidation products is an order of magnitude larger than those reported by *Krechmer et al.* [2016]. Chamber operating conditions can be excluded as the main source of discrepancy based on the measurements during the Focused Isoprene eXperiment at the California Institute of Technology campaign; see Figures S4 and S7 in *Krechmer et al.* [2015]. We tentatively attribute this discrepancy between the behavior of the two chambers to possible line losses and different ionization schemes of the two Chemical Ionization Mass Spectrometers (CIMS) that were used. The extent to which the CIMS design impacts measured vapor wall loss rates requires additional study.

3.2. Effect of Seed Composition on Oxidation State of Aerosols

As shown in Figure 1, $\overline{OS_C}$ in SN-seeded experiments exceeded those with AS seed particles. AMS calibration experiments performed by atomizing solutions of pinic acid mixed with either SN or AS revealed that the $\overline{OS_C}$ of the aerosol mixtures are the same, regardless of the seed (Figure S3). The use of nitrate aerosols does not introduce a bias on the elemental ratios.

Positive matrix factorization (PMF) analysis was performed to investigate the reasons for the observed higher $\overline{OS_C}$ in SN- versus AS-seeded experiments, as PMF analysis has been shown to differentiate wall loss, vapor-particle partitioning, and chemical conversion [*Craven et al.*, 2012]. For the high AS experiment, three PMF factors were resolved (Figure 4b; also see PMF analysis in Text S6). Factor 1_{H_SO4}, the most oxygenated factor, dominates early in the oxidation, suggesting the prompt formation of low-volatility organics. As the reaction proceeds, accumulation of less oxygenated SVOCs (Figure 3), identified in offline samples, is favored [*Zhang et al.*, 2015a]. The temporal profiles of the PMF factors and the offline-detected products suggest that the prompt partitioning of ELVOCs followed by the partitioning of SVOCs onto the growing aerosol results in an initial decrease of $\overline{OS_C}$ in α-pinene SOA (Figure 5a). Under low/medium AS surface area experiments, only 2 factors with O:C ratios similar to the semivolatile factors in high-AS surface area experiments are resolved (Figure S4c). A highly oxidized factor such as factor 1_{H_SO4} was not resolved in lower AS surface area experiments, likely owing to the accelerated loss of ELVOCs to the wall, resulting in lower mass concentrations of the particle-phase ELVOCs.

In the high SN-seeded experiment, the initial partitioning of highly oxygenated species (factor 1_{H_NO3}; $\overline{OS_C}$ = 0.2) followed by the less oxygenated ones (factor 2_{H_NO3}; $\overline{OS_C}$ = −0.23) resulted in the early decrease of $\overline{OS_C}$. In contrast to factor 3_{H_SO4} in the high-AS experiment, which represents the least oxygenated species,

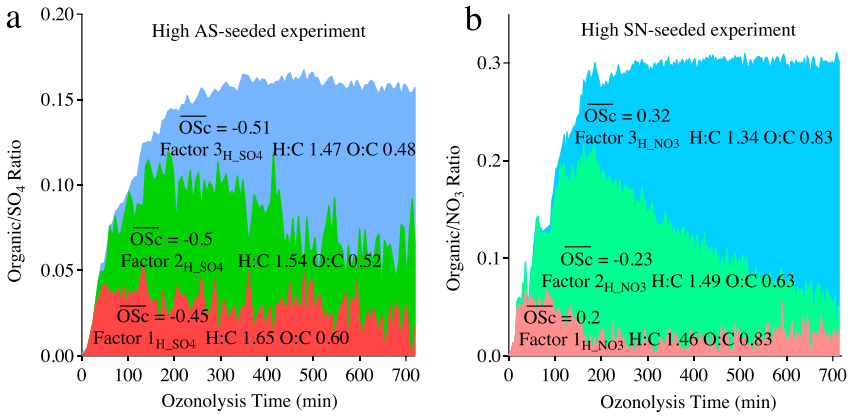

Figure 4. Temporal profiles for organic-to-inorganic ratios of three PMF resolved OA factors in high (a) AS- and (b) SN-seeded experiments.

factor 3_{H_NO3} in the high-SN experiment is a highly oxidized factor with particle $\overline{OS_C}$ of 0.32. Contribution of factor 3_{H_NO3} to the total PMF-resolved organic mass started to increase significantly at 200 min, where a plateau of total organic mass was reached, to about 80% at 720 min. Meanwhile, factors 1_{H_NO3} and 2_{H_NO3} decreased without any significant change of the overall PMF-resolved organic/inorganic ratio. PMF analysis suggests that the first condensed species may have been converted to the highly oxidized species factor 3_{H_NO3} in the particle phase.

We further compare the molecular composition of α-pinene SOA produced in the presence of AS versus SN seed particles. Seventeen molecular products, with average $\overline{OS_C}$ of -0.5, were identified by offline UPLC/MS analysis, and these products account for $>50\%$ of the α-pinene SOA mass under high aerosol loadings [*Zhang et al.*, 2015a]. However, the relative abundances of these products in the presence of AS versus SN seed particles are quite similar, as shown in Figure 3. To our knowledge, only a few classes of species exhibit positive $\overline{OS_C}$ that could potentially elevate the overall oxidation state of α-pinene SOA in the presence of SN seeds. The highly oxidized organic molecules (HOMs; $\overline{OS_C} > 0$) produced through the autoxidation chemistry have been widely observed in the α-pinene + O_3 system [e.g., *Ehn et al.*, 2014]. Due to their rapid production rates and extremely low volatilities, they account for an important source of SOA during initial particle growth [*Kirkby et al.*, 2016]. As more semivolatile oxidation products condense onto the seed particles, the fraction of HOMs starts to decrease and thus cannot explain the factor 3_{H_NO3} revealed from PMF analysis.

Another important class of species with positive $\overline{OS_C}$ is small carboxylic acids. Our GC/MS analysis of α-pinene SOA samples suggests that acetic acid ($\overline{OS_C} = 0$) is present in all the offline samples (Figure S7). In addition, we found that the $C_xH_yO_z^+$ ion intensity increases over the entire course of the high SN-seeded experiment

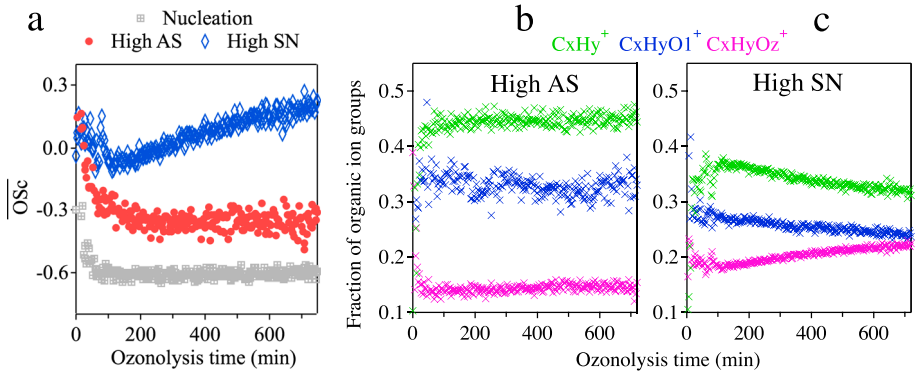

Figure 5. (a) $\overline{OS_C}$ in high AS-seeded, SN-seeded, and nucleation experiments. Temporal profiles of $C_xH_y^+$, $C_xH_yO_1^+$ and $C_xH_yO_z^+$ ion groups in (b) high AS-seeded and (c) high SN- seeded experiments.

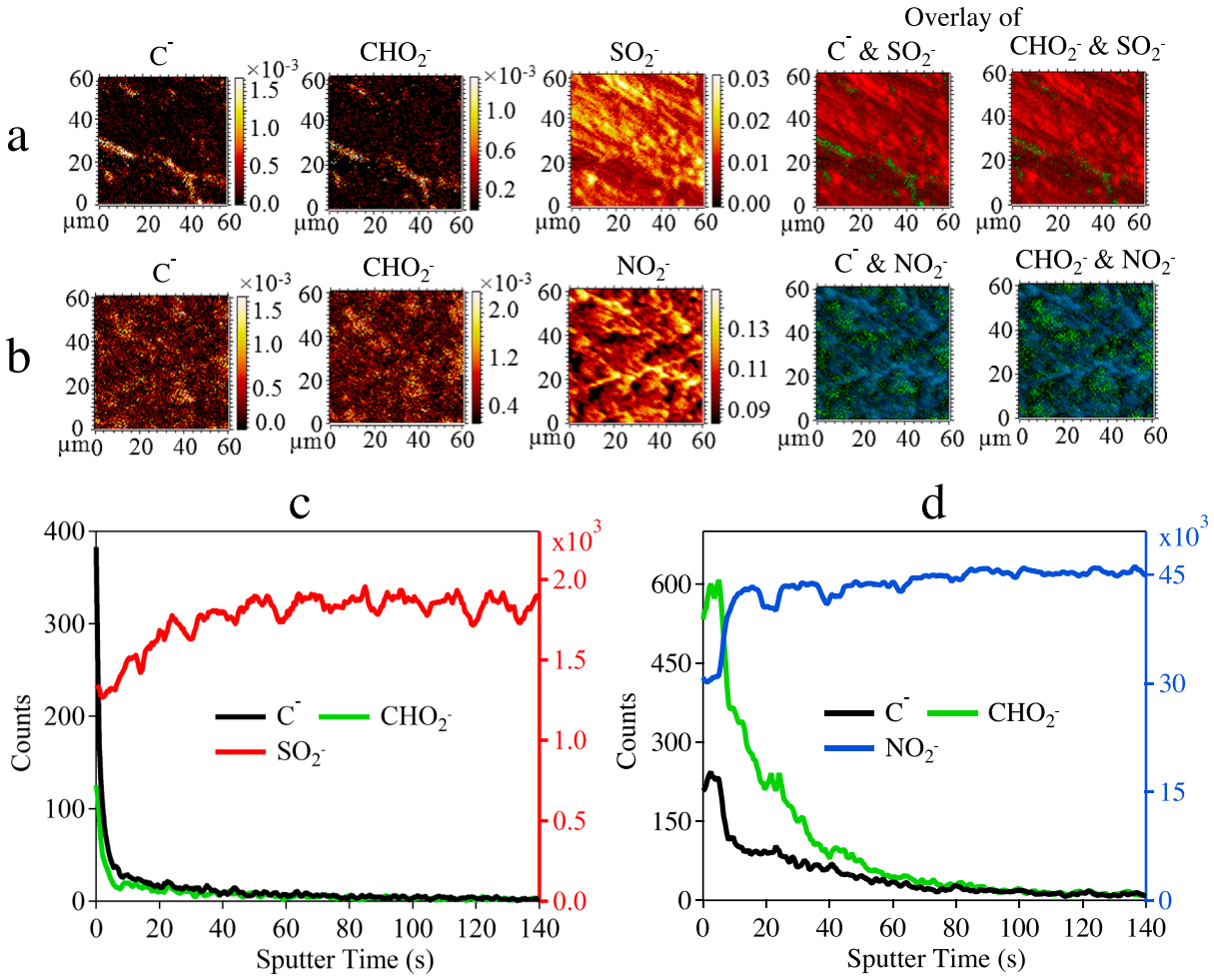

Figure 6. (a and b) ToF-SIMS images of AS particles and SN particles, respectively, after the total 200 s sputtering. ToF-SIMS images were normalized to the total intensity. The color scales represent the normalized signal intensities of C^- and CHO_2^-, representing carboxylic acids, and SO_2^- and NO_2^-, representing AS and SN, respectively. The overlaid images show the distribution and coverage of the organic (green) on the surface of AS (red) and SN (blue). (c and d) depth profiles reconstructed from the areas indicated in Figures 6a and 6b, respectively. The sputtering time is an indicator of the sputtering depth assuming the sputtering rates for AS and SN particles are the same.

(Figure 5c). The CO_2^+ ion, the characteristic fragment of carboxylic acids, contributes ~87% of the total $C_xH_yO_z^+$ ion intensity in the high SN-seeded experiment (Figure S8). These results are consistent with previous observations of the presence of formic, acetic, and pyruvic acids with $\overline{OS_C}$ of 2, 0, and 0.7, respectively, in α-pinene ozonolysis SOA [*Kidd et al.*, 2014; *Koch et al.*, 2000; *Lee et al.*, 2006; *Orlando et al.*, 2000].

Altogether, the lagged increase of a highly oxidized factor in the PMF results, the higher oxidation state of SOA, and the presence of small highly oxidized carboxylic acid in SN particles suggests that nitrate-containing salts may promote SOA aging and increase SOA oxidation state by retaining highly oxygenated small acids. This observation is consistent with increasing evidence [*Shilling et al.*, 2006; *Shilling and Tolbert*, 2004; *Wang and Laskin*, 2014; *Wang et al.*, 2015] of carboxylic acid-nitrate particle-phase or multiphase vapor-particle reactions, forming low-volatility inorganic salts. Further surface analysis of particles upon uptake of acetic acid provided additional evidence of the enhanced uptake of small acids on SN particles versus AS particles by offline ToF-SIMS.

3.3. Surface Analysis of SN and AS Particles After Uptake of Acetic Acid

To examine the potential interactions between small carboxylic acids and SN particles, we conducted uptake experiments using acetic acid as a proxy for the small carboxylic acids. A custom-made stainless steel reaction cell with an internal volume of around 30 mL was used, as illustrated in Figure S9 [*Wu et al.*, 2007]. The

deposited inorganic materials were dried under high-purity N_2 for >2 h before being exposed to acetic acid vapor. Details of flow cell experiments and ToF-SIMS operation are given in Text S4. Figures 6a and 6b show the negative ion images of the AS and SN particles, respectively, after 200 s of sputtering. The C^- and CHO_2^- ions were selected to represent acetic acid, and the SO_2^- and NO_2^- ions were chosen to represent the AS and SN particles, respectively. ToF-SIMS ion images clearly show the presence of acetic acid on the AS and SN particles, suggesting a higher acetic acid coverage on the surface of the SN particles than that of the AS particles. Figures 6c and 6d show the depth profiles of selected ions, which could be used to estimate the relative thicknesses of the acetic acid layer on the surface of the AS and SN particles assuming that the sputtering rates for both particles were similar. The organic signal of the AS surface (green and black lines) decreased to a very small value within 10 s, while the inorganic sulfate signal (red line) sharply increased (Figure 6c). For the SN surface, the organic signal decreased more gradually and became small only after more than 100 s of sputtering (Figure 6d) indicating that the acetic acid layer on the SN surface was much thicker than that on the AS surface and the surface of SN particles might be much rougher. The uptake experiments were carried out several times to ensure the repeatability of the results. The results are consistent with previous work showing that nitrate particles can efficiently uptake highly oxidized low molecular weight carboxylic acids at low temperatures, i.e., 240 K, even when particles are effloresced [*Shilling et al*., 2006; *Shilling and Tolbert*, 2004].

4. Summary and Conclusions

We report studies of the formation of SOA from α-pinene + O_3 under two different seed aerosol types, ammonium sulfate (AS) and sodium nitrate (SN) at four different seed aerosol concentrations (one of which is absence of seed, i.e., particle formation by nucleation). We find that for both AS and SN seed particles, $\overline{OS_C}$ increases with increasing seed surface area, consistent with increasing condensation of extremely low volatility SOA-forming species. We also observed increased O:C atomic ratios, by as much a factor of 2, in the presence of concentrated SN seed particles. Positive matrix factorization (PMF) analysis, molecular constituents' identification, and organic thickness measurements were further performed to explore the main factors contributing to the unexpectedly high SOA oxidation state. Our results suggest that nitrate-containing seed particles could potentially increase the overall degree of oxygenation of SOA by retaining highly oxidized small acids.

Acknowledgments
This work was funded by the HKUST Sponsorship scheme for Targeted Strategic Partnerships and U.S. National Science Foundation grant AGS-1523500. Data used to generate the figures are available upon request.

References

Canagaratna, M. R., et al. (2015), Elemental ratio measurements of organic compounds using aerosol mass spectrometry: Characterization, improved calibration, and implications, *Atmos. Chem. Phys.*, *15*(1), 253–272, doi:10.5194/acp-15-253-2015.

Craven, J. S., et al. (2012), Analysis of secondary organic aerosol formation and aging using positive matrix factorization of high-resolution aerosol mass spectra: Application to the dodecane low-NO_x system, *Atmos. Chem. Phys.*, *12*(24), 11,795–11,817, doi:10.5194/acp-12-11795-2012.

Ehn, M., et al. (2014), A large source of low-volatility secondary organic aerosol, *Nature*, *506*(7489), 476–479, doi:10.1038/nature13032.

Gaston, C. J., T. P. Riedel, Z. Zhang, A. Gold, J. D. Surratt, and J. A. Thornton (2014), Reactive uptake of an isoprene-derived epoxydiol to submicron aerosol particles, *Environ. Sci. Technol.*, *48*(19), 11,178–11,186, doi:10.1021/es5034266.

Hao, L.-q., Z.-y. Wang, M.-q. Huang, L. Fang, and W.-j. Zhang (2007), Effects of seed aerosols on the growth of secondary organic aerosols from the photooxidation of toluene, *J. Environ. Sci.*, *19*(6), 704–708, doi:10.1016/S1001-0742(07)60117-X.

Jang, M., N. M. Czoschke, S. Lee, and R. M. Kamens (2002), Heterogeneous atmospheric aerosol production by acid-catalyzed particle-phase reactions, *Science*, *298*(5594), 814–817, doi:10.1126/science.1075798.

Jang, M., B. Carroll, B. Chandramouli, and R. M. Kamens (2003), Particle growth by acid-catalyzed heterogeneous reactions of organic carbonyls on preexisting aerosols, *Environ. Sci. Technol.*, *37*(17), 3828–3837, doi:10.1021/es021005u.

Kidd, C., V. Perraud, and B. J. Finlayson-Pitts (2014), New insights into secondary organic aerosol from the ozonolysis of alpha-pinene from combined infrared spectroscopy and mass spectrometry measurements, *Phys. Chem. Chem. Phys.*, *16*(41), 22,706–22,716, doi:10.1039/C4CP03405H.

Kirkby, J., et al. (2016), Ion-induced nucleation of pure biogenic particles, *Nature*, *533*(7604), 521–526, doi:10.1038/nature17953.

Koch, S., R. Winterhalter, E. Uherek, A. Kolloff, P. Neeb, and G. K. Moortgat (2000), Formation of new particles in the gas-phase ozonolysis of monoterpenes, *Atmos. Environ.*, *34*(23), 4031–4042, doi:10.1016/S1352-2310(00)00133-3.

Krechmer, J. E., et al. (2015), Formation of low volatility organic compounds and secondary organic aerosol from isoprene hydroxyhydroperoxide low-NO oxidation, *Environ. Sci. Technol.*, *49*(17), 10,330–10,339, doi:10.1021/acs.est.5b02031.

Krechmer, J. E., D. Pagonis, P. J. Ziemann, and J. L. Jimenez (2016), Quantification of gas-wall partitioning in Teflon environmental chambers using rapid bursts of low-volatility oxidized species generated in situ, *Environ. Sci. Technol.*, *50*(11), 5757–5765, doi:10.1021/acs.est.6b00606.

Kroll, J. H., et al. (2011), Carbon oxidation state as a metric for describing the chemistry of atmospheric organic aerosol, *Nat. Chem.*, *3*(2), 133–139, doi:10.1038/nchem.948.

Lee, A., A. H. Goldstein, M. D. Keywood, S. Gao, V. Varutbangkul, R. Bahreini, N. L. Ng, R. C. Flagan, and J. H. Seinfeld (2006), Gas-phase products and secondary aerosol yields from the ozonolysis of ten different terpenes, *J. Geophys. Res.*, *111*, D07302, doi:10.1029/2005JD006437.

Lu, Z., J. Hao, H. Takekawa, L. Hu, and J. Li (2009), Effect of high concentrations of inorganic seed aerosols on secondary organic aerosol formation in the m-xylene/NO_x photooxidation system, *Atmos. Environ.*, *43*(4), 897–904, doi:10.1016/j.atmosenv.2008.10.047.

Mai, H. J., M. Shiraiwa, R. C. Flagan, and J. H. Seinfeld (2015), Under what conditions can equilibrium gas-particle partitioning be expected to hold in the atmosphere? *Environ. Sci. Technol.*, *49*(19), 11,485–11,491, doi:10.1021/acs.est.5b02587.

McVay, R. C., X. Zhang, B. Aumont, R. Valorso, M. Camredon, Y. S. La, P. O. Wennberg, and J. H. Seinfeld (2016), SOA formation from the photooxidation of α-pinene: Systematic exploration of the simulation of chamber data, *Atmos. Chem. Phys.*, *16*, 2785–2802, doi:10.5194/acp-16-2785-2016.

Nguyen, T. B., M. M. Coggon, K. H. Bates, X. Zhang, R. H. Schwantes, K. A. Schilling, C. L. Loza, R. C. Flagan, P. O. Wennberg, and J. H. Seinfeld (2014), Organic aerosol formation from the reactive uptake of isoprene epoxydiols (IEPOX) onto non-acidified inorganic seeds, *Atmos. Chem. Phys.*, *14*(7), 3497–3510, doi:10.5194/acp-14-3497-2014.

Orlando, J. J., B. Noziere, G. S. Tyndall, G. E. Orzechowska, S. E. Paulson, and Y. Rudich (2000), Product studies of the OH- and ozone-initiated oxidation of some monoterpenes, *J. Geophys. Res.*, *105*, 11,561–11,572, doi:10.1029/2000JD900005.

Pieber, S. M., et al. (2016), Inorganic salt interference on CO_2^+ in aerodyne AMS and ACSM organic aerosol composition studies, *Environ. Sci. Technol.*, doi:10.1021/acs.est.6b01035.

Shilling, J. E., and M. A. Tolbert (2004), Uptake of acetic acid on thin ammonium nitrate films as a function of temperature and relative humidity, *J. Phys. Chem. A*, *108*(51), 11,314–11,320, doi:10.1021/jp046135z.

Shilling, J. E., B. M. Connelly, and M. A. Tolbert (2006), Uptake of small oxygenated organic molecules onto ammonium nitrate under upper tropospheric conditions, *J. Phys. Chem. A*, *110*(21), 6687–6695, doi:10.1021/jp055940q.

Sioutas, C. (2004), Personal particle monitor, Google Patents.

Surratt, J. D., M. Lewandowski, J. H. Offenberg, M. Jaoui, T. E. Kleindienst, E. O. Edney, and J. H. Seinfeld (2007), Effect of acidity on secondary organic aerosol formation from isoprene, *Environ. Sci. Technol.*, *41*(15), 5363–5369, doi:10.1021/es0704176.

Wang, B. B., and A. Laskin (2014), Reactions between water-soluble organic acids and nitrates in atmospheric aerosols: Recycling of nitric acid and formation of organic salts, *J. Geophys. Res. Atmos.*, *119*, 3335–3351, doi:10.1002/2013JD021169.

Wang, B. B., R. E. O'Brien, S. T. Kelly, J. E. Shilling, R. C. Moffet, M. K. Gilles, and A. Laskin (2015), Reactivity of liquid and semisolid secondary organic carbon with chloride and nitrate in atmospheric aerosols, *J. Phys. Chem. A*, *119*, 4498–4508, doi:10.1002/2013JD021169.

Wu, H. B., M. N. Chan, and C. K. Chan (2007), FTIR characterization of polymorphic transformation of ammonium nitrate, *Aerosol Sci. Technol.*, *41*(6), 581–588, doi:10.1080/02786820701272038.

Zhang, X., C. D. Cappa, S. H. Jathar, R. C. Mcvay, J. J. Ensberg, M. J. Kleeman, and J. H. Seinfeld (2014), Influence of vapor wall loss in laboratory chambers on yields of secondary organic aerosol, *Proc. Natl. Acad. Sci. U.S.A.*, *111*(16), 5802–5807, doi:10.1073/pnas.1404727111.

Zhang, X., R. C. McVay, D. D. Huang, N. F. Dalleska, B. Aumont, R. C. Flagan, and J. H. Seinfeld (2015a), Formation and evolution of molecular products in α-pinene secondary organic aerosol, *Proc. Natl. Acad. Sci. U.S.A.*, *112*(46), 14,168–14,173, doi:10.1073/pnas.1517742112.

Zhang, X., R. H. Schwantes, R. C. McVay, H. Lignell, M. M. Coggon, R. C. Flagan, and J. H. Seinfeld (2015b), Vapor wall deposition in Teflon chambers, *Atmos. Chem. Phys.*, *15*(8), 4197–4214, doi:10.5194/acp-15-4197-2015.